Desalination and Water Treatment
www.deswater.com
doi: 10.1080/19443994.2014.886298

54 (2015) 1044–1053
April

Taylor & Francis
Taylor & Francis Group

Kinetics of electro-Fenton ferrous regeneration (EFFR) on chlorinated organic compound degradation

Thanakorn Methatham[a,b,c,*], Ming-Chun Lu[d], Chavalit Ratanatamskul[e]

[a]*Department of Environmental Engineering, Faculty of Engineering, Khon Kaen University, 40002 Khon Kaen, Thailand*
Email: thanakorn@kku.ac.th
[b]*Research Center for Environmental and Hazardous Substance Management, Faculty of Engineering, Khon Kaen University, 40002 Khon Kaen, Thailand*
[c]*Center of Excellence on Hazardous Substance Management (HSM), Khon Kaen University Branch, 40002 Khon Kaen, Thailand*
[d]*Department of Environmental Resources Management, Chia Nan University of Pharmacy and Science, 717 Tainan, Taiwan*
[e]*Department of Environmental Engineering, Faculty of Engineering, Chulalongkorn University, 10330 Bangkok, Thailand*

Received 18 November 2013; Accepted 12 January 2014

ABSTRACT

The electro-Fenton ferrous regeneration (EFFR) process was studied for kinetic determination under various reaction conditions. A novel model equation of this process was proposed which uses 2,4-dichlorophenol (2,4-DCP) as a chlorinated organic reference for this study. The operating parameters, pH, electrical current densities, and hydrogen peroxide concentrations, were varied to validate this novel model and kinetic rate constant estimation. The kinetic rate constant of the hydroxyl radical (·OH) with 2,4-DCP obtained by the novel model from this experiment was between 6.76×10^9 and 7.82×10^9 $M^{-1}s^{-1}$. As a result, the novel model showed a more suitable fit with the experimental data than the first-order model method. The goodness of data fit which were indicated by correlation coefficients r^2 demonstrated that the novel model can better describe the kinetics of the process for chlorinated organic compound oxidation than the first-order model. Hydroquinone, maleic, acetic, formic, and oxalic acids were the main oxidation intermediates in this experiment. A degradation pathway for chlorinated organic compound oxidation by EFFR process was proposed on the basis of the intermediate compounds detected.

Keywords: Electro-Fenton ferrous regeneration (EFFR); Chlorinated organic compound; Novel kinetic model; First-order model; Hydroxyl radicals

1. Introduction

Recently, chlorinated organic compounds have been the subject of greater attention due to their environmental significance as potentially hazardous substances. One of the priority chlorinated organic pollutants listed by the US is EPA, 2,4-dichlorophenol (2,4-DCP), which has been widely employed in many industrial processes [1]. 2,4-DCP has also been found in disinfected water following chlorination, in the flue

*Corresponding author.

Presented at the 6th International Conference on the "Challenges in Environmental Science and Engineering" (CESE-2013), 29 October–2 November 2013, Daegu, Korea

gas of municipal waste incineration, and in pulp and paper wastewaters [2,3]. From previous studies, 2,4-DCP is believed to be the cause of some abnormalities in the human endocrine system including some pathological symptoms [4,5]. Advanced oxidation processes (AOPs), which involve the generation of highly reactive and non-selective hydroxyl radicals (·OH), can be used to destroy hazardous and refractory organic pollutants in surface and groundwater in and industrial wastewater. It has been well proven that a variety of refractory organics can be effectively degraded by the ·OH generated by the Fenton reaction [6,7]. The combined technologies of AOPs, an electrochemical regeneration system with Fenton's reagents, have been developed using electrochemically induced original Fenton's reagents and proposed as an alternative method for organic removal. However, while most combined technologies of AOPs in the electrochemical system in cooperation with Fenton's reagents have been studied with the primary focus on the kinetics of the electro-generation of H_2O_2 type, the electro-regeneration of Fe^{2+} type or electro-Fenton ferrous regeneration (EFFR) has largely been neglected.

Although the first-order model is commonly used to describe kinetics, there are some limitations to precisely describing the process apart from the initial reaction period of the Fenton and electro-Fenton processes [8]. A second-order kinetic model is also widely used to describe the kinetics of electrochemical combination with Fenton's reagents, where the degradation of 2,4-dichlorophenoxyacetic acid in an aqueous solution was used in the study of Wang and Lemley [9]. However, it could describe only the kinetics of the anodic Fenton process. Another method, which is a competitive technique, is also known to be more accurate than the first-order model method, only it has to be determined together with using the original substances [10]. Though the competition kinetics have given much kinetic data for hydroxyl radicals through various applications, such as Fenton reaction, photolysis of H_2O_2, photo-Fenton reaction, and ozone reactions, neither hydroxyl radicals nor the reaction products could be measured directly [11]. In addition to the above-mentioned methods, a study by Anotai et al. [12] on kinetic determination compared the kinetics of aniline degradation using Fenton and electro-Fenton reactions in terms of the overall rate of equation for aniline degradation. However, the outcome of this method was in a reaction order of 1.1 through Fenton's reaction (almost a first-order reaction) and a reaction order of 0.46 through the electro-Fenton reaction (about a half-order reaction). In other studies, the first-order model was applied to describe the kinetics in terms of the total organic carbons [13,14] of the reaction in electrochemical combination with Fenton's reagents process as well as representing the kinetic constants in each phase of the overall reaction period when divided into two or three phases [15]. In order to discover a good kinetic model to describe the electrochemical combination with Fenton's reagents reaction, some key factors are not to be overlooked such as the concentration of hydrogen peroxide and ferrous ion, and the current density. Although there have been studies on the oxidation of organic compounds and hydroxyl radicals, none of the reports could attest to the kinetics of the EFFR process. This research proposes a novel kinetic model of EFFR and verifies the kinetic model for use to find the kinetics of chlorinated organic degradation by hydroxyl radicals in the EFFR process, in which 2,4-DCP was used as the chlorinated organic compounds' representative. After that, the kinetic rate constant was estimated and calculated according to the mathematical formulas of the novel kinetic model.

2. Materials and methods

2.1. Material for experiments

All chemicals used were of high purity grade from Merck. The 2,4-DCP was dissolved in de-ionized water (millipore system with a resistivity of 18.2 $M\Omega\,cm^{-1}$) to create the synthetic wastewater containing 1 mM of 2,4-DCP. The pH was adjusted and controlled by the pH controller for the addition of H_2SO_4 or NaOH as required.

The experiments on EFFR kinetic investigation were conducted in a $15 \times 20 \times 20$ cm acrylic reactor containing 5 liters of working volume. The mesh-type titanium metal coating with IrO_2/RuO_2 electrodes was used as the anode and the stainless steel electrodes were used as the cathode. A constant electrical current from a DC power supply was discharged to all electrodes in the process. Two mixers were equipped to generate complete agitation in the reactor. The temperature of the system was maintained at a constant 25°C by a thermal controller. A calculated amount of catalytic ferrous sulfates of 0.1 mM was added as the source of Fe^{2+} in this experiment. H_2O_2 of 1–5 mM was added afterwards into the reactor at a flow rate of 0.5 mL min^{-1} in the function of continuous feeding with the power supply turned on to start the reaction. The concentrations of 2,4-DCP, Fe^{2+}, and H_2O_2 were measured and controlled to validate the novel kinetic model of the process with 20 min selected time intervals. The samples taken at selected times were instantly injected into the NaOH

solution containing tubes to immediately stop further reaction by increased pH of 11 for iron precipitation [16]. Then, the samples were immediately filtered through a 0.45 m micro-filter syringe to separate precipitated iron from the solution.

2.2. Analytical method for experiment

The concentration of 2,4-DCP was determined by a high-performance liquid chromatograph (HPLC) (Thermo Scientific Model) with an equipped UV detector (Finnigan Spectra SYSTEM UV1000). The separation column is a reverse-phase column (Shodex Asahipak, ODP-50 6D 4.6 × 250 mm, 5 m) with a mobile phase that consists of acetonitrile, water, and acetic acid at a particular ratio (69:30:1). The H_2O_2 concentration was measured by a spectrophotometer (Shimadzu UV-1201) at 400 nm wavelength, using $K_2Ti(C_2O_4)_3$ (analytical grade) as an indicator. The ferrous concentration was determined according to the Standard Methods (APHA, 1992) by light absorbance measurement at 510 nm after complex with 1,10-phenanthroline using a UV–vis spectrophotometer [16]. HPLC and Ion Chromatograph (IC) (Dionex DX-120) equipped with RFC-30 EGCII (KOH), IonPac® AG 11 guard column (4 × 50 mm), IonPac® AS11 analytical column (4 × 250 mm), ASRS®-ULTRA II (4 mm) suppressor, and conductivity detector were used to identify the intermediates that might be present during the reactions while the results were confirmed by gas chromatography using a mass spectrophotometer (GC-MS) to propose the reaction pathways. All experimental scenarios were duplicated.

2.3. Proposed novel kinetic modeling for electro-Fenton ferrous regeneration (EFFR) process

The basic reaction of the EFFR process should involve three key reactions: the generation of Fe^{2+} from Fe^{3+} on the surface of the cathode (Reaction R1), the generation of hydroxyl radicals (·OH) between Fe^{2+} and H_2O_2 (Reaction R2), and the degradation of organic substance by the ·OH (Reaction R5). Some reversed reactions and side reactions (Reactions R3, R4, R6, and R7) coexist simultaneously with the key reactions as summarized below [17–19]:

$$Fe^{3+} + e^- \xrightarrow{k_1} Fe^{2+} \quad \text{(R1)}$$

$$Fe^{2+} + H_2O_2 \xrightarrow{k_2} Fe^{3+} + {\cdot}OH + OH^- \quad \text{(R2)}$$

$$Fe^{2+} + {\cdot}OH \xrightarrow{k_3} Fe^{3+} + OH^- \quad \text{(R3)}$$

$$Fe^{3+} + H_2O_2 \xrightarrow{k_4} Fe^{2+} + HO_2^{\cdot} + H^+ \quad \text{(R4)}$$

$${\cdot}OH + \text{organic} \xrightarrow{k_5} \text{products} \quad \text{(R5)}$$

$$H_2O_2 + \text{organic} \xrightarrow{k_6} \text{products} \quad \text{(R6)}$$

$${\cdot}OH + H_2O_2 \xrightarrow{k_7} HO_2^{\cdot} + H_2O \quad \text{(R7)}$$

The novel kinetic model for describing the EFFR process can be determined by assuming that the organic substance (S) is primarily degraded by ·OH and its reaction rate ($d[S]/dt$) can be supposed by Eq. (1):

$$-\left[\frac{d[S]}{dt}\right] = k_5[{\cdot}OH][S] \quad (1)$$

From the reactions R2, R3, R5, and R7, the adjustment of ·OH concentration ($d[{\cdot}OH]/dt$) in relation to its generation rate from H_2O_2 and Fe^{2+}, and its consumption rate of reaction with Fe^{2+}, organic substance, and H_2O_2 are shown below:

$$\frac{d[{\cdot}OH]}{dt} = k_2[Fe^{2+}][H_2O_2] - k_3[Fe^{2+}][{\cdot}OH] - k_5[{\cdot}OH][S] - k_7[{\cdot}OH][H_2O_2] \quad (2)$$

Moreover, the results of many studies have supported the assertion that ·OH is a highly reactive free radical with an extremely short lifetime of nanoseconds [20]. Its concentration is usually considered to be constant but only at a low level and the $d[{\cdot}OH]/dt$ approaches zero according to a steady-state approximation. Then, Eq. (1) can be rearranged in terms of organic degradation rate, becoming a function of $[H_2O_2]$ and [S] mainly, as Eq. (3):

$$-\left[\frac{d[S]}{dt}\right] = k_5[S]\left(\frac{k_2[Fe^{2+}][H_2O_2]}{k_3[Fe^{2+}] + k_7[H_2O_2] + k_5[S]}\right) \quad (3)$$

The concentration of Fe^{2+} in the system is dependent on its regeneration rate at the cathode (Reaction R1) and the decomposition rate (reaction R2 and R3). It can be inferred that there is a relationship between the

rate of Fe^{2+} concentration and the current applied (I) on the cathode; so it can be expressed by Eq. (4).

$$\frac{d[Fe^{2+}]}{dt} = k_1 I[Fe^{3+}] - k_2[Fe^{2+}][H_2O_2] - k_3[Fe^{2+}][\cdot OH] + k_4[Fe^{3+}][H_2O_2] \quad (4)$$

Assuming that the $[H_2O_2]$ during the reaction is proportional to its initial concentration $[H_2O_2]_0$ with a fixed ratio of α, with the initial condition at $t = 0$, $[Fe^{2+}] = [Fe^{2+}]_0$, $[Fe^{2+}]$ can be shown and expressed as Eq. (6).

$$\frac{d[Fe^{2+}]}{dt} = (k_1 I\lambda - k_2\alpha[H_2O_2]_0)[Fe^{2+}] \quad (5)$$

$$[Fe^{2+}] = [Fe^{2+}]_0 e^{(k_1 I\lambda - k_2\alpha[H_2O_2]_0)t} \quad (6)$$

The above equation indicates that $[Fe^{2+}]$ is a function of experimental time. It was demonstrated that $[Fe^{2+}]$ in this system depends on the factors of I and $[H_2O_2]_0$. Once we use Eq. (6) to replace Eq. (2), the rate of organic degradation can be further expressed as follows:

$$-\frac{d[S]}{dt} = k_5[S]\left(\frac{k_2[Fe^{2+}]}{k_3\frac{[Fe^{2+}]}{[H_2O_2]} + k_7 + k_5\frac{[S]}{[H_2O_2]}}\right) \quad (7)$$

After integration, the organic or chlorinated organic concentration [S] becomes a function of experimental time, decreasing from its initial concentration $[S_0]$ at the beginning of the reaction ($t = 0$) gradually as described by Eq. (8).

$$\ln\frac{[S_0]}{[S]} + \frac{k_5}{(k_3[Fe^{2+}]_0 + k_7\alpha[H_2O_2]_0)}([S_0] - [S]) = \frac{k_5 k_2[Fe^{2+}]_0}{(k_3\left(\frac{[Fe^{2+}]_0}{[H_2O_2]_0}\right) + k_7)(k_1\lambda I - k_2\alpha[H_2O_2]_0)} (e^{(k_1\lambda I - k_2\alpha[H_2O_2]_0)t} - 1) \quad (8)$$

To simplify Eq. (8), let

$A = k_5/(k_3[Fe^{2+}]_0 + k_7\alpha[H_2O_2]_0)$,

$B = k_5 k_2[Fe^{2+}]_0/(k_3([Fe^{2+}]_0/[H_2O_2]_0)+k_7)(k_1\lambda I - k_2\alpha[H_2O_2]_0)$ and

$C = k_1\lambda I - k_2\alpha[H_2O_2]_0$,

The above equation can be rearranged to a simplified form as shown below in Eq. (9).

$$\ln\frac{[S_0]}{S} + A([S_0] - [S]) = B(e^{Ct} - 1) \quad (9)$$

From the rate equation [Eq. (3)], term A in Eq. (9) can be derived using the modification of the inverse of the initial graphical method [21], or obtained from the intercept/slope of graphical plot as shown below.

$$r = -\frac{d[S]}{dt} = k_5[S]\left(\frac{k_2[Fe^{2+}][H_2O_2]}{k_3[Fe^{2+}] + k_7[H_2O_2] + k_5[S]}\right) \quad (9a)$$

$$\frac{1}{r} = \frac{1}{\text{initial rate}} = \frac{t}{1 - \frac{[s]}{[s_0]}} = \left(\frac{k_3[Fe^{2+}] + k_7[H_2O_2]}{k_5 k_2[Fe^{2+}][H_2O_2]}\right)\frac{1}{[S]} + \frac{1}{k_2[Fe^{2+}][H_2O_2]} \quad (9b)$$

The ferrous mechanism equation [Eq. (6)] can be adapted to a natural logarithm as shown in equation (9c) for finding the term C from slope which is shown below:

$$\ln\frac{[Fe^{2+}]}{[Fe^{2+}]_0} = (k_1\lambda I - k_2\alpha[H_2O_2]_0)t \quad (9c)$$

In conclusion, the novel kinetic equations (Eqs. (9), (9a), (9b), and (9c)) have been established as the main kinetic model for the EFFR process to describe the kinetics of organic degradation in an aqueous solution against reaction time and also with the performance of Fe^{2+} regeneration.

2.4. Experimental model setup

To validate and establish the novel kinetic model, the assumptions were as follows:

(1) The solution in the reactor was mixed completely.
(2) The temperature was constant at 25°C.
(3) Fe^{2+} was the dominant form of Fe(II) species at pH 2.6–3.0 [22]. The change of pH was omitted as the maximum variation of 0.05 and was allowed throughout the process.
(4) The hydroxyl radical was the main radical to attack all organic substances in the solution. H_2O_2, $HO_2^{\cdot}$, and O_2^{-} were unable to degrade the contaminant.
(5) The resistance at anode and cathode electrodes was so minimal that it can be disregarded.

The validation was done in three sets of experiments that used 2,4-DCP as the chlorinated organic representative. Three sets of experiments were conducted to study the effect of operating pH, current density, and hydrogen peroxide concentration. All of the experiments were compared with both the first-order kinetic model and our novel model.

3. Results and discussion

3.1. Effect of different operating pH on electro-Fenton ferrous regeneration (EFFR) kinetics

Hydroxyl radical productivity and the concentration of ferrous ions were controlled by the pH of the solution. Hence, pH is an important parameter for the EFFR process also. It is well known that the reaction of both Fenton and EFFR processes have the highest efficiency when the pH is around 2–4 [23]. In this experiment, constant pH values of 2, 3, and 3.5 were used for investigating the effect of pH on EFFR kinetics. The experiment was conducted using both the first-order kinetic model and the novel model for kinetic constant determination as shown in Fig. 1. The results of both models indicated that pH 3 was the best condition in 2,4-DCP removal by the EFFR process with confirmation by a higher initial degradation rate than other pH values reported in Table 1. As can be seen in Table 1, the results indicate that the rate constant depended on the pH of the solution. At pH over 3.0, the decreasing oxidation potential of ·OH affected the reduction of the decomposition rate, and also the increasing of pH induced a decrease in the fraction of dissolved iron species. While at pH under 3.0, the electro-generated hydrogen peroxide solvates a proton to form an oxonium ion ($H_3O_2^+$) which enhances its stability and reduces the reactivity with ferrous ions, and consequently less hydroxyl radicals are produced by reaction 2 [24].

3.2. Effect of current density on electro-Fenton ferrous regeneration (EFFR) kinetics

One of the important parameters that affect the EFFR process is the amount of DC current supplied to the electrodes [25]. The experimental condition of initial Fe^{2+} 0.1 mM and H_2O_2 1 mM with continuous feeding at constant pH 3 was performed to study the effect of current densities on the kinetics of the process. The current density, 0.01, 0.05, 0.10, 0.25, and 0.50 mA cm^{-2}, was varied to investigate the effect of current density on the amount of ferrous concentration and the kinetics of the process. The ferrous concentration remaining ratio in terms of natural logarithm [Ln (Fe^{2+}/Fe_0^{2+})] depended significantly on the current density as shown in Fig. 2. The results also show that a higher ferrous concentration remaining ratio was found when increasing current density caused the higher current force to support the continuous regeneration of [Fe^{3+}] to [Fe^{2+}] in the system according to the theory of current efficiency and the Faraday laws mentioned by Quiang et al. [26]. The rate constant of 2,4-DCP with hydroxyl radical in various conditions of current density variation was determined by data plotted compared to the first-order model as shown in Fig. 3, and using Equation 9 with the novel model analysis as reported in Table 2. The rate constants obtained from various current densities were found to be in the range of 6.99×10^9–7.33×10^9 $M^{-1}s^{-1}$. The data from Table 2 indicate that when current density increased, our novel model (plotted [$Ln(S_0/S)+A(S_0-S)$] vs. [e^{Ct}-1]) could give higher correlation coefficients compared to the former first-order model. This suggests that the novel model is suitable

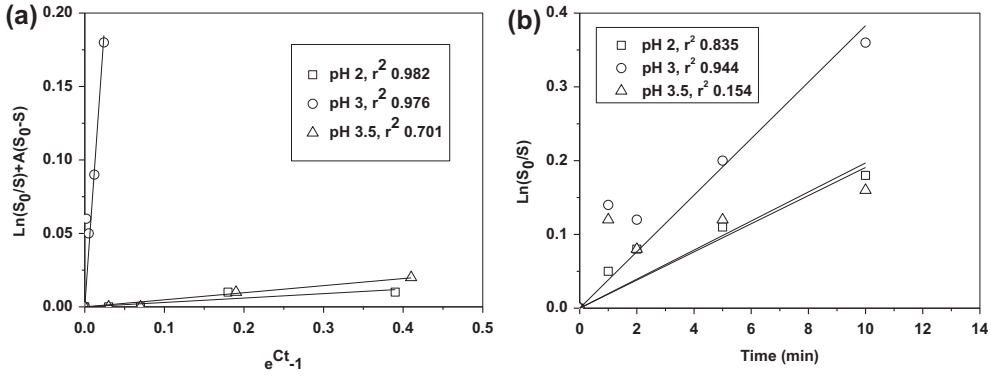

Fig. 1. Effect of various constant pH on novel kinetic model (a) and first-order model (b) plotted ([2,4-DCP] 1 mM, [Fe^{2+}] 0.1 mM, [H_2O_2] 1 mM, and electrical current density 0.05 mA cm^{-2}).

Table 1
Effect of pH on kinetic constant ([2,4-DCP] 1 mM, [Fe^{2+}] 0.1 mM, [H_2O_2] 1 mM (continuous feed), and electrical current 0.05 mA cm^{-2})

pH	Initial degradation rate (10^{-3} mM min^{-1})	k (1st-order) (min^{-1})	$k_{.OH \rightarrow 2,4\text{-DCP}}$ (novel model) (10^9 M^{-1} s^{-1})
2.0	19.5	0.0195	6.07
3.0	34.4	0.0344	7.05
3.5	18.9	0.0189	6.05

Note: All data were calculated at 10 min of reaction time.

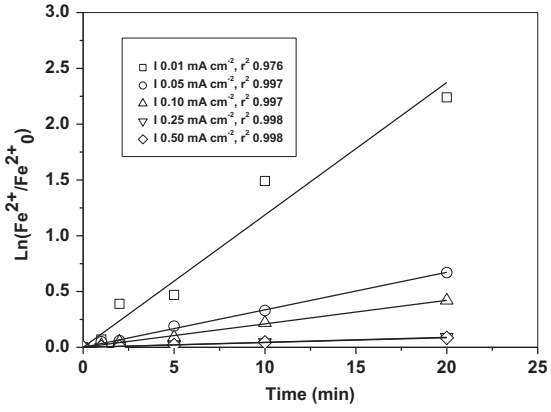

Fig. 2. Effect of various current densities on ferrous concentration remaining ratio ([2,4-DCP] 1 mM, [Fe^{2+}] 0.1 mM, [H_2O_2] 1 mM, pH 3, and electrical current 0.01–0.50 mA cm^{-2}).

and better for kinetic investigation than the first-order model for the EFFR process since the current density is also considered a significant parameter to be included in EFFR kinetic determination.

3.3. Effect of hydrogen peroxide concentration on electro-Fenton ferrous regeneration (EFFR) kinetics

The most important reagent playing the role of an oxidizing agent in Fenton and also in EFFR processes is hydrogen peroxide (H_2O_2). For this experiment, H_2O_2 concentration was varied to determine the relationship between the amount of ferrous concentration remaining and the kinetics in the electrochemical regeneration of Fenton's reagents process. Ferrous concentration (Fe^{2+}) of 0.1 mM and current density of 0.05 and 0.10 mA cm^{-2} were used at constant pH 3, and H_2O_2 was continuously fed at different total concentrations of 1, 3, and 5 mM for the kinetic investigation experiment. The experiment was studied using both the first-order kinetic model and our novel model together. The relationship between H_2O_2 concentrations and the amount of Fe^{2+} remaining is shown in Fig. 4. The result of the Fe^{2+} remaining ratio in this process suggests that increasing H_2O_2 concentration could affect the rate constant of ferrous concentration remaining (C) as shown in Table 2. The data of H_2O_2 variation in Table 2 shows that an initial degradation rate of 2,4-DCP removal and ferrous concentration remaining constant were due to an increase in hydroxyl radical concentration resulting from H_2O_2 addition. However, at a higher dosage of H_2O_2 with current density increasing, the degradation rate was decreased because the hydroxyl radicals were scavenged by the effect of H_2O_2 (Reaction 7) and the recombination of the hydroxyl radicals. It can be seen that higher rates of 2,4-DCP degradation and ferrous regeneration were achieved when optimum H_2O_2 concentration was used. The rate constants obtained from various H_2O_2 concentrations were plotted for the novel model and compared with the first-order model as shown in Figs. 5 and 6. The rate constants for vari-

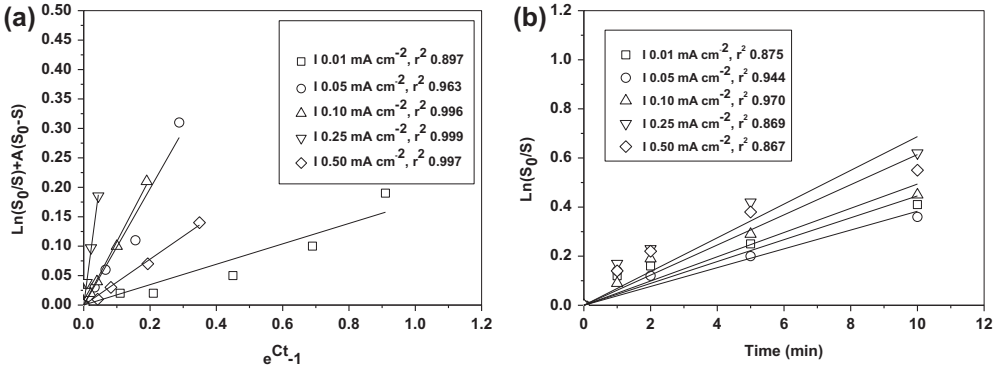

Fig. 3. Effect of various current densities on novel kinetic model (a) and first-order model (b) plotted ([2,4-DCP] 1 mM, [Fe^{2+}] 0.1 mM, [H_2O_2] 1 mM, pH 3, and electrical current 0.01–0.50 mA cm^{-2}).

Table 2
The summary of the rate constant of 2,4-DCP with hydroxyl radical estimation by novel model under various conditions

Fe^{2+} (mM)	H_2O_2 (mM)	Current density (mA cm^{-2})	Initial degradation rate (10^{-3} mM min^{-1})	C	$k_{\cdot OH \rightarrow 2,4\text{-DCP}}$ (novel model) (10^9 M^{-1} s^{-1})	r^2 (novel model)	r^2 (pseudo 1st-order model)
0.1	1	0.01	34.0	0.119	7.23	0.897	0.875
		0.05	34.4	0.034	7.05	0.963	0.944
		0.10	45.9	0.021	7.33	0.996	0.970
		0.25	68.3	0.004	7.12	0.999	0.869
		0.50	61.3	0.042	6.99	0.997	0.867
0.1	1	0.05	34.4	0.002	7.07	0.976	0.944
	3		64.3	0.052	7.29	0.986	0.970
	5		78.3	0.001	7.36	0.948	0.976
0.1	1	0.10	45.9	0.009	7.75	0.983	0.970
	3		67.6	0.095	7.82	0.885	0.827
	5		56.4	0.006	6.76	0.988	0.821

Note: All of the data were calculated at 20 min of reaction time.

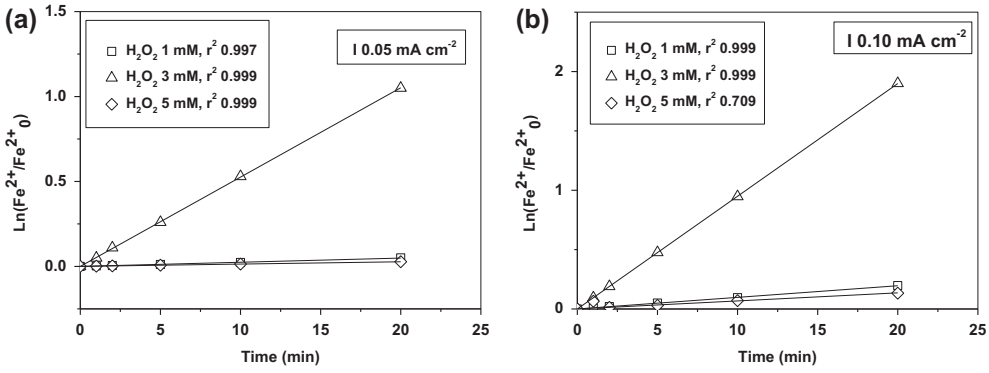

Fig. 4. Effect of various H_2O_2 on ferrous concentration remaining ratio plotted ([2,4-DCP] 1 mM, [Fe^{2+}] 0.1 mM, [H_2O_2] 1–5 mM, pH 3, electrical current 0.05 (a) and 0.10 (b) mA cm^{-2}).

ous H_2O_2 concentrations were found to be between 6.76×10^9 and 7.82×10^9 $M^{-1}s^{-1}$ as shown in Table 2. The data from the table show that at low current density with different H_2O_2 concentrations, the linear correlation coefficients in the novel model gave a fit similar to the first-order model. However, it seemed to better fit the novel model than the first-order model when a higher current density was applied. This suggests that the rate constant of the EFFR process depends significantly on H_2O_2 concentrations and also current density. All data confirm that the novel model is a good application for determining the hydroxyl radical kinetic rate constant of the EFFR process.

3.4. Rate constant estimation of 2,4-DCP as chlorinated organic compound representative with hydroxyl radical

With reference to the novel model expressed in Eq. (9), the rate constant of 2,4-DCP used as an organic representative with hydroxyl radical is summarized in Table 2. As shown in the results table, the rate constants ranged from 6.76×10^9 to 7.82×10^9 $M^{-1}s^{-1}$ which was similar to the data of the kinetic constant of ·OH and 2,4-DCP by Fenton process reported by Tang and Huang [27]. The model was also validated by the experiments on the degradation of 2,4-DCP as an organic representative at a concentration of Fe^{2+} 0.1 mM, H_2O_2 1–5 mM (continuous feeding), and constant pH 3 with different current densities (0.01, 0.05, 0.10, 0.25, and 0.50 mA cm^{-2}). For the model performance comparison, the experimental data were plotted using both our novel model and the first-order model, respectively. Table 2 presents the fitting results in linear form for our novel model and the first-order model. Apparently, the correlation coefficients for the fitting of our novel model are significantly greater than those of the first-order model. Although the conventional first-order model is the simplest model to describe the variety of chemical

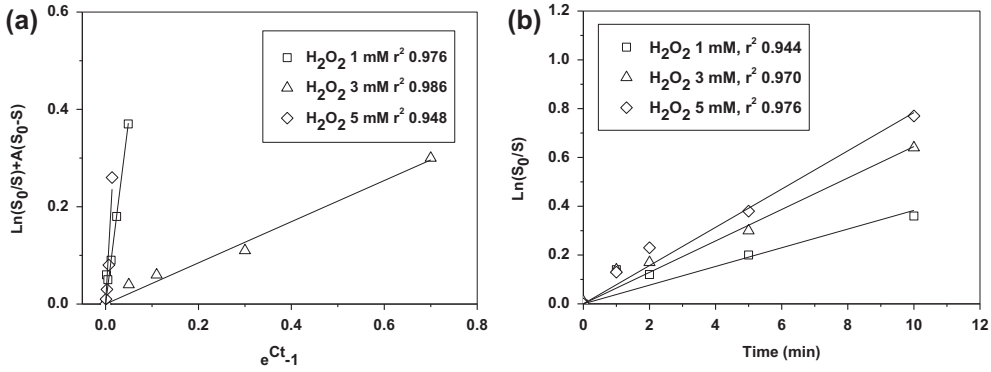

Fig. 5. Effect of various H_2O_2 on novel kinetic model (a) and first-order model (b) plotted ([2,4-DCP] 1 mM, [Fe^{2+}] 0.1 mM, [H_2O_2] 1–5 mM, pH 3, and electrical current 0.05 mA cm^{-2}).

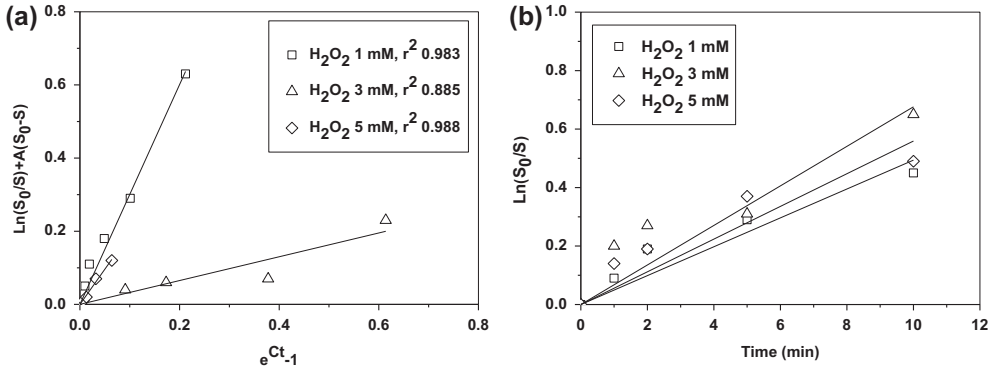

Fig. 6. Effect of various H_2O_2 on novel kinetic model (a) and first-order model (b) plotted ([2,4-DCP] 1 mM, [Fe^{2+}] 0.1 mM, [H_2O_2] 1–5 mM, pH 3, and electrical current 0.10 mA cm^{-2}).

reactions and has been widely applied to various water and wastewater treatment processes, it is difficult to accurately describe the kinetics of the EFFR reaction precisely. It should be noted that the novel model can clearly identify the kinetics of EFFR and that the prediction in organic degradation and the phenomena of the process can be derived more accurately than the first-order model.

3.5. Proposed reaction pathways and mechanisms

The evolution of the aromatic intermediates of 2,4-DCP degradation by EFFR process is illustrated in Fig. 7. HPLC and IC were applied to identify the intermediates that might occur among the reactions which were then confirmed by GC-MS. The results showed that the evolution of only one aromatic intermediate hydroquinone was shown to increase in the first minute of the experiment. In this experiment, the highest concentration of hydroquinone was detected at 2 min. It decreased to close to zero at near 10 min. The results showed that the group of carboxylic acids started to generate in the initial minutes of process reaction time and increased to maximum concentration in this experiment following 10 min and possibly decreased after that. Maleic acid and acetic acid were the earlier and more abundant products of the carboxylic acid group at the initial stage. It can be inferred that these compounds are the primary products indicator of the ring cleavage of aromatic intermediates. Acetic acid, oxalic acid, and formic acid were generated at the time around 10 min, similar to the maleic acid evolution. These are the most successive organic products prior to conversion to CO_2 which accumulated in the solution. This implies that under the studied condition, within 90 min of reaction time, 2,4-DCP could be almost completely mineralized to CO_2. This is in agreement with the total organic carbon profile of initial organic carbon being converted to CO_2. Considering the carbon balance at the

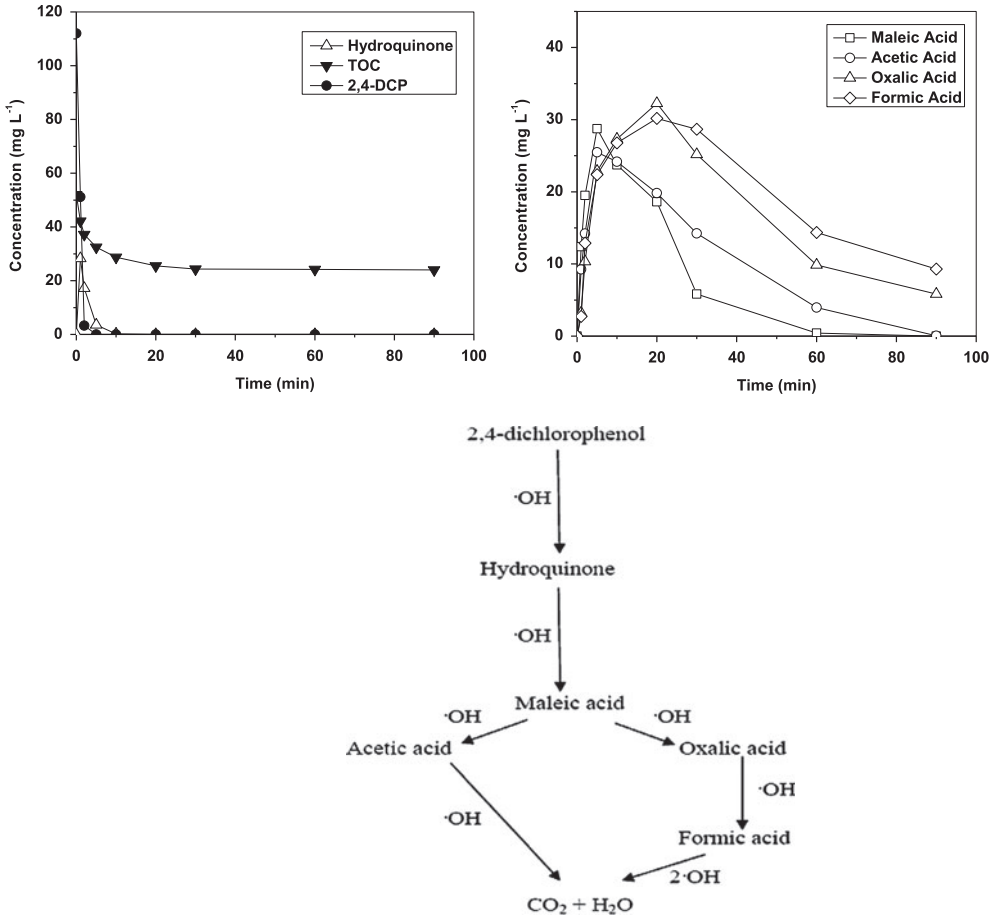

Fig. 7. Proposed reaction pathway and intermediates evolution for 2,4-DCP degradation by the electro-Fenton ferrous regeneration (EFFR) process. ([2,4-DCP] 1 mM, [Fe^{2+}] 0.1 mM, [H_2O_2] 3 mM, pH 3, and electrical current 0.10 mA cm^{-2}).

end of the reaction period, it can be seen that more than 50% of the organic carbon could be quantified from the identified intermediates.

The reaction pathways of 2,4-DCP oxidation by the EFFR process was proposed in this study. The degradation pathway, as shown in Fig. 7, was proposed as follows: 2,4-DCP was found to oxidize directly to hydroquinone and further be oxidized to the formation of aliphatic carboxylic acid directly; it was confirmed that an ·OH steady state was generated in the experiment which could only occur from the continuous H_2O_2 feeding condition. These phenomena suggest that the continuous H_2O_2 feeding condition may help prevent the toxic compound forms which might be generated under the original feeding condition. The ring cleavage resulted in the formation of maleic acid and the degradation could be further separated into two directions. The first direction is into the acetic acid formation. The second direction is into the oxalic acid and formic acid formation by hydrogen abstraction. In both degradation pathways, carbon dioxide and water were directly produced as the final products.

4. Conclusion

In this study, a novel model of kinetic determination is proposed. The rate constant of reaction between 2,4-DCP as chlorinated organic compounds and •OH obtained by our novel model was reported between 6.76×10^9 and 7.82×10^9 $M^{-1}s^{-1}$. All data confirmed that the novel model could be applied for the EFFR rate constant determination and could clearly identify the kinetics of EFFR. Also, the prediction in organic degradation and phenomena of process could be derived more accurately than the first-order model. However, the novel model has only been validated by the experiments of 2,4-DCP degradation thus far. Further studies to apply this kinetic model in the

degradation of other organics and chlorinated organics are necessary. Finally, the degradation pathway for 2,4-DCP degradation by the EFFR process was also proposed on the basis of intermediate compounds detected.

Acknowledgment

This research was supported by the 90th Ratchadaphiseksomphoch Funds from Chulalongkorn University, Research Funds from the Faculty of Engineering, Khon Kaen University, the Research Center for Environmental and Hazardous Substance Management Funds, Khon Kaen University, and the Center of Excellence on Hazardous Substance Management Funds from Khon Kaen University, Thailand.

References

[1] W.Z. Tang, C.P. Huang, 2,4-dichlorophenol oxidation kinetics by Fenton's reagent, Environ. Technol. 17 (1996) 1371–1378.
[2] N.V. Heeb, I.S. Dolezal, T. Bührer, P. Mattrel, M. Wolfensberger, Distribution of halogenated phenols including mixed brominated and chlorinated phenols in municipal waste incineration flue gas, Chemosphere 31 (1995) 3033–3041.
[3] M. Pérez, F. Torrades, J.A. García-Hortal, X. Domènech, J. Peral, Removal of organic contaminants in paper pulp treatment effluents under Fenton and photo-fenton conditions, Appl. Catal., B 36 (2002) 63–74.
[4] A. Handan, O. Nurullah, U. Nuray, Investigation of the accumulation of 2,4-dichlorophenoxyacetic acid (2,4-D) in rat kidneys, Forensic Sci. Int. 153 (2005) 53–57.
[5] J.F. Zhang, H. Liu, Y.Y. Sun, X.R. Wang, J.C. Wu, Y.Q. Xue, Responses of the antioxidant defenses of the Goldfish Carassius auratus, exposed to 2,4-dichlorophenol, Environ. Toxicol. Pharmacol. 19 (2005) 185–190.
[6] J.P. Joseph, Dark and photo assisted Fe^{3+}-catalyzed degradation of chlorophenoxyherbicides by hydrogen peroxide, Environ. Sci. Technol. 26 (1992) 944–951.
[7] E. Oliveros, O. Legrini, M. Hohl, T. Müller, A.M. Braun, Industrial waste water treatment: Large scale development of a light-enhanced Fenton reaction, Chem. Eng. Process. 36 (1997) 397–405.
[8] B. Gözmen, M.A. Oturan, N.O. Oturan, O. Erbatur, Indirect electrochemical treatment of bisphenol A in water via electrochemically generated Fenton's reagent, Environ. Sci. Technol. 37 (2003) 3716–3723.
[9] Q.Q. Wang, A.T. Lemley, Kinetic model and optimization of 2,4-D degradation by anodic Fenton treatment, Environ. Sci. Technol. 35 (2001) 4509–4514.
[10] N. Boonrattanakij, M.C. Lu, J. Anotai, Kinetics and mechanism of 2,6-dimethyl-aniline degradation by hydroxyl radicals, J. Hazard. Mater. 172 (2–3) (2009) 952–957.
[11] B.G. Kwon, S. Ryu, J. Yoon, Determination of hydroxyl radical rate constants in a continuous flow system using competition kinetics, J. Ind. Eng. Chem. 15 (6) (2009) 809–812.
[12] J. Anotai, M.C. Lu, P. Chewpreecha, Kinetics of aniline degradation by Fenton and electro-Fenton processes, Water Res. 40 (2006) 1841–1847.
[13] E. Brillas, R. Sauleda, J. Casado, Degradation of 4-chlorophenol by anodic oxidation, Electro-Fenton, photoelectro-Fenton, and peroxi-coagulation processes, J. Electrochem. Soc. 145 (1998) 759–765.
[14] E. Brillas, J.C. Calpe, J. Casado, Mineralization of 2,4-D by advanced electrochemical oxidation processes, Water Res. 34 (2000) 2253–2262.
[15] W. Chu, C.Y. Kwan, K.H. Chan, S.K. Kam, A study of kinetic modelling and reaction pathway of 2,4-dichlorophenol transformation by photo-fenton-like oxidation, J. Hazard. Mater. 121 (2005) 119–126.
[16] N. Masomboon, C. Ratanatamskul, M.-C. Lu, Chemical oxidation of 2,6-dimethylaniline by electrochemically generated Fenton's reagent, J. Hazard. Mater. 176 (2010) 92–98.
[17] C. Walling, Fenton's reagent revisited, Acc. Chem. Res. 8 (1975) 125–131.
[18] W.P. Ting, M.-C. Lu, Y.-H. Huang, Kinetics of 2,6-dimethylaniline degradation by electro-Fenton process, J. Hazard. Mater. 161 (2009) 1484–1490.
[19] E. Neyens, J. Baeyens, A review of classic Fenton's peroxidation as an advanced oxidation technique, J. Hazard. Mater. 98 (2003) 33–50.
[20] D.X. Liu, J. Liu, J. Wen, Elevation of hydrogen peroxide after spinal cord injury detected by using the Fenton reaction, Free Radical Biol. Med. 27 (1999) 478–482.
[21] M.J. Liou, M.C. Lu, Catalytic degradation of nitroaromatic explosives with Fenton's reagent, J. Mol. Catal. A: Chem. 277 (2007) 155–163.
[22] N. Kang, D.S. Lee, J. Yoon, Kinetic modeling of Fenton oxidation of phenol and monochlorophenols, Chemosphere 47 (2002) 915–924.
[23] C.K. Duesterberg, S.E. Mylon, T.D. Waite, pH effects on iron-catalyzed oxidation using Fenton's reagent, Environ. Sci. Technol. 42 (2008) 8522–8527.
[24] B.G. Kwon, D.S. Lee, N. Kang, J. Yoon, Characteristics of p-chlorophenol oxidation by Fenton's reagent, Water Res. 33 (1999) 2110–2118.
[25] J.-L. Chen, J.-Y. Wang, C.-C. Wu, K.-Y. Chiang, Electrocatalytic degradation of 2,4-dichlorophenol by granular graphite electrodes, Colloids Surf., A 379 (1-3) (2011), 163–168.
[26] Z. Qiang, J.-H. Chang, C.-P. Huang, Electrochemical regeneration of Fe2+ in Fenton oxidation processes, Water Res. 37 (2003) 1308–1319.
[27] W.Z. Tang, C.P. Huang, Effect of chlorine content of chlorinated phenols on their oxidation kinetics by Fenton's reagent, Chemosphere 33 (1996) 1621–1635.